Journal Teknologi

Full Paper

SEISMIC PERFORMANCE OF HORIZONTALLY IRREGULAR CONCRETE BUILDINGS: A PUSHOVER ANALYSIS APPROACH

Yuyun Tajunnisa[a]*, Ibnu Pudji Rahardjo[a], Hazen Masrafat[b], Aliyyah Putri Ramaditya[a], Vonny Nur Halisah[a]

[a]Departement of Civil Infrastructure Engineering, Institut Teknologi Sepuluh Nopember, Surabaya, Indonesia
[b]Departement of Civil Engineering, Universitas Negeri Gorontalo, Gorontalo, Indonesia

Article history
Received
20 November 2024
Received in revised form
26 May 2025
Accepted
26 May 2025
Published Online
27 February 2026

*Corresponding author
yuyun_t@its.ac.id

Abstract

Irregular building configurations, both horizontally and vertically, are more vulnerable to seismic forces, requiring careful evaluation to reduce the risk of structural collapse. This study investigates the seismic performance of three horizontally irregular building models: Model A (U-shaped), Model B (L-shaped), and Model C (T-shaped). Nonlinear static pushover analysis is used to assess structural performance, covering collapse levels, displacement, drift ratio, and base shear, validated by SNI 1726-2019 and referencing FEMA 356 and ATC-40 for performance point evaluation. Pushover analysis simulates the building's behavior under lateral forces, identifying the performance point where the structure transitions to inelastic behavior. The results show that Model A (U-shaped) has the largest displacements (5.15% in the X-direction and 4.92% in the Y-direction) and the highest drift ratios (5.02% in the X and 4.61% in the Y) due to greater torsional eccentricity. Base shear values for Model A are also higher (5.32% for X and 7.60% for Y). According to FEMA 356, Model A achieves an "Immediate Occupancy" classification, while ATC-40 places it under "Damage Control." This study highlights the importance of detailed pushover analysis in designing seismic-resistant irregular buildings.

Keywords: Horizontal Irregularity, Pushover Analysis, SDG 9 (Industry, Innovation, Infrastructure), Seismic Performance, Structural Performance

1.0 INTRODUCTION

The construction industry's rapid evolution has led to numerous asymmetrical building configurations, primarily driven by aesthetic considerations. In Indonesia, the construction of both regular and irregular multi-story buildings poses significant seismic risks that necessitate rigorous structural performance evaluations. However, the substantial damage observed in past seismic events underscores the critical need to comprehensively evaluate existing structures to mitigate risks to human life and socio-economic stability [1]. Seismic analysis for such buildings must employ spatial models considering multidirectional seismic effects, specifically the simultaneous action of at least two horizontal ground motion components [2]. The inadequate seismic resistance of many existing buildings, stemming from insufficient understanding and practical application of earthquake-resistant design, has contributed to structural failures under seismic or cyclic loading conditions (fatigue) [3]. According to IS 2893:2016 [4], a structure is classified as irregular when it exhibits an uneven distribution of geometric configurations, including vertical setbacks, re-entrant corners, mass irregularity, or stiffness irregularity. Structural weaknesses, commonly concentrated in specific areas, increase the likelihood of localized damage that may propagate into overall collapse. Such vulnerabilities often manifest in insufficient floor strength, stiffness, or mass distribution [5]. Existing seismic design codes address vertical and horizontal irregularities, emphasizing the need for refined performance-based analysis to ensure structural

integrity and serviceability throughout the building's life span [6].

Structural irregularities require a more performance design analysis to maintain buildings' existing functions. Previous research has assessed the seismic performance of regular and irregular multi-story buildings using the SNI 03-1726-2012 code through equivalent static analysis methods. [7][8]. However, structural performance evaluation using the equivalent static analysis method has limitations, as it cannot estimate the maximum forces and deformations that occur, nor can it identify the critical or damaged parts of the structure. Alternatively, structural performance can be assessed by evaluating the extent of damage or potential collapse of the structure under the design-level earthquake. Structural failure can be identified through nonlinear static analysis, considering the inelastic behavior of the structure. The performance of each building's structure exhibits different values for the same intensity of load, considering performance levels, displacement, drift ratio, and base shear. [9].

Recent seismic studies on irregular buildings have significantly increased, focusing on the pushover analysis method to assess seismic performance. [10][11] [12]. FEMA 356 (2000) and ATC-40 (1996) guidelines are widely referenced for structural performance and retrofitting of buildings under seismic load [13][14][15]. Finite element analysis (FEA) and nonlinear dynamic analysis (NDA) are used to model seismic loading situations and assess how structures respond to various abnormalities. Structural capacity and dynamic properties are evaluated using analytical approaches such as pushover analysis and modal analysis. Pushover analysis is a static and nonlinear procedure in which the magnitude of lateral forces is gradually increased while maintaining a predetermined distribution pattern along the height of the building. [16]. The pushover curve provides basic information about a building's seismic performance and is a powerful tool for evaluating seismic behavior based on a displacement-based strategy. According to the displacement-based design approach, defining the seismic performance level is necessary, which is related to the level of damage exhibited by the structure and is usually identified through strain or drift limits. [17]. While substantial literature has analyzed pushover methods, most studies focus on vertical irregularities or regular building configurations. Very few have explored horizontal irregularities, such as U-shaped, L-shaped, and T-shaped buildings, which are commonly found in seismic-prone areas. Compared to regular buildings, these configurations introduce mass and stiffness distributions that can significantly amplify torsional effects and structural deformation.

Studied the impact of geometrical irregularity on seismic performance and noted that higher torsional eccentricity increases displacement and structural damage [18]. However, this study primarily focused on multi-story buildings with re-entrant corners. It did not explicitly compare various models with horizontal irregularities like U-shaped, L-shaped, and T-shaped configurations. This study aims to bridge this gap by analyzing the pushover analysis of these three horizontally irregular building models and comparing performance points, base shear, displacement, and drift ratios across these configurations.

In addition, [6] Analyzed the effects of horizontal irregularity on building performance, finding that such buildings exhibit increased shear forces and deformation, leading to higher structural damage. However, their research was limited to specific structural models and did not delve into comparing more complex irregular building configurations. [19] Provided insight into irregular building behavior using pushover analysis. Still, they did not investigate more complex horizontal irregular configurations or consider the torsional eccentricity effects in U-shaped buildings, which are crucial for a more comprehensive understanding of seismic behavior.

This study thus offers a novel contribution by focusing on horizontal irregularity and the torsional effects it causes, specifically comparing U-shaped, L-shaped, and T-shaped buildings with regular configurations. It aims to evaluate the seismic performance of these models using pushover analysis and further extends the understanding of torsional eccentricity, plastic hinge formation, and displacement under seismic loading conditions. By integrating these factors, the study provides a deeper insight into irregular buildings' structural vulnerabilities and performance levels, offering an advanced approach to seismic design and retrofitting in seismic-prone regions.

2.0 METHODOLOGY

2.1 Example Buildings and Material Properties

This study analyzed the performance level of irregular horizontal structures, comparing them with regular structures (Figure 1). Three variation shape models of the horizontal irregular structures (Figure 2-Figure 4) were analyzed. The selection of U-shaped (Model A), L-shaped (Model B), and T-shaped (Model C) building configurations was based on common irregular building layouts observed in actual urban developments, especially in healthcare facilities and commercial buildings. These configurations often result from functional spatial requirements such as circulation flow, zoning for medical services, emergency access routes, and architectural aesthetics. According to case studies and damage reports from past earthquakes in Indonesia and worldwide, buildings with re-entrant corners (as in U and L shapes) or intersecting wings (as in T shapes) exhibit significant torsional irregularities and stress concentrations, making them more vulnerable under seismic loading. Previous research, such as by Pandian *et al*. (2024) [5] and Divya and Murali (2022) [20], highlighted these configurations as critical for seismic assessment due to their higher eccentricities and

complex load paths. Therefore, these models were chosen to represent realistic, high-risk typologies in seismic-prone regions. This study's building structures functioned as hospitals with reinforced concrete structure types. All models of regular and irregular buildings have the same area of 600 m² and 10 stories (37 meters). In addition, all the model buildings' structural design and material properties are the same. The structural design of this study is presented in Table 1, whereas Table 2 presents the material properties considered in the design.

Table 1 Structural design of example building

Stories	Slab(mm)	Beams		Column	
		Width (mm)	Depth (mm)	Width (mm)	Depth (mm)
Roof	100	400	500	-	-
10	120	400	500	700	700
9	120	400	500	700	700
8	120	500	600	700	700
7	120	500	600	800	800
6	120	500	600	800	800
5	120	600	700	800	800
4	120	600	700	900	900
3	120	600	700	900	900
2	120	600	700	900	900
1	-	-	-	1000	1000

Table 2 Material properties of the design of example building

Material properties	Concrete	Steel
Compressive strength (MPa)	25	-
Yield strength (MPa)	-	420
Modulus of elasticity (MPa)	2350	200000
Mass per unit volume (kN/m3)	24	78.50

2.2 Model Limitations

This study, while aiming to assess the seismic performance of horizontally irregular buildings realistically, is subject to several modeling limitations that must be acknowledged:

- **Uniform Material Properties**: The models employ idealized and uniform material properties for concrete and reinforcement. Variations in construction quality, material aging, or degradation over time are not considered, which may affect actual performance during seismic events.
- **Geometry Modeling and Irregularities:** The U-, L-, and T-shaped building configurations represent typical horizontal irregularities in real buildings; however, these remain idealized models. Other factors were not included, such as floor heights, stiffness variations from shear walls or internal partitions, and vertical irregularities.
- **Load Assumptions and Load Combinations**: Dead and live loads follow SNI 1727-2020, and seismic loads follow SNI 1726-2019. However, seismic dynamic loads are modeled using response spectrum and nonlinear static pushover analyses, idealized approaches compared to time-history dynamic simulations. These limits are in understanding the structural response under complex earthquake time histories.
- **Joint and Structural Element Modeling:** The model assumes rigid and perfect connections between structural elements without considering potential joint degradation or nonlinear behavior at plastic hinge locations.
- **Analysis Under Initial Undamaged Conditions:** All models are assumed to be initially free of defects or damage.
- **Exclusion of Environmental and Additional Loads** Environmental factors such as temperature changes, humidity, and additional loads like wind are not considered, and the analysis is focused solely on seismic response.

2.3 Analysis Methods

Building analysis was conducted using SAP2000 v.24 software. The analysis began with a linear dynamic analysis using the response spectrum method to determine the structural response to seismic loads. Static loads, including dead load and live load, were calculated based on Indonesian National Standard SNI 1727-2020 [21], while the seismic load was considered according to Indonesian National Standard SNI 1726-2019 [22]. The load combinations considered in this study followed SNI 1726-2019, specifically:

- 1.4 Dead Load (D) + 1.7 Live Load (L)
- 1.2 Dead Load (D) + 1.6 Live Load (L) + 0.5 Earthquake Load (E)
- 1.2 Dead Load (D) + 1.0 Earthquake Load (E) + 1.0 Live Load (L)
- 0.9 Dead Load (D) + 1.0 Earthquake Load (E).

These combinations were selected to capture both the ultimate limit states and serviceability limit states under the influence of gravity and seismic loads. Subsequently, nonlinear pushover analysis was conducted in two loading stages to evaluate the structural performance of the building under gravity loads and lateral thrust loads.

Stage I: Gravity Loads

In the first stage, the building structure was subjected to gravity loads, which include dead loads with a load factor of 1.0 and live loads with a load factor of 0.3. The analysis considers nonlinear conditions in this stage, including the structure's behavior under gravity loads. Finite Element Analysis (FEA) was used to accurately represent the behavior of structural elements, including the nonlinear relationship between stress and strain in the material.

Stage II: Lateral Thrust Load (Pushover)

In the second stage, lateral thrust loads were applied to the structure using static nonlinear pushover

analysis. This stage begins once the first stage is completed, where the initial condition option Continue from State at the end of Nonlinear Case is activated, meaning the final condition of the gravity analysis in Stage I serves as the starting point for Stage II analysis. The lateral loads are defined as acceleration loads for X-direction and Y-direction loading. In Stage II, lateral loads were applied step-by-step in a monotonically nonlinear static analysis. [23]. This process is carried out in SAP2000 by defining Load Cases through the Define-Load Cases-Add New Cases menu, named PUSH-X and/or PUSH-Y, with the analysis type set to Static Nonlinear. In this stage, lateral load patterns are applied gradually to the structure, with the lateral forces increasing monotonically until the target displacement, set at 2% of the building height, is achieved. [14].

Defining Hinge Properties (Plastic Hinge)

After defining the lateral thrust loads, the next step is determining the Hinge Properties for the beams and columns. The hinge definition is carried out separately by filling in the Hinge Frame Assignment and Auto Hinge Assignment Data for each involved structural element. Hinge overwrites are also configured, meaning that plastic hinges are assumed to occur at approximately 2% of the frame length being analyzed. This definition allows the model to accurately depict inelastic behavior in structural elements that undergo plastic deformation under seismic loading. Using the plastic hinge model, the analysis can identify weak points and failure modes within the structure, such as excessive deformation or local damage that may develop into overall structural collapse.

Pushover analysis provides crucial information regarding the seismic performance of the building, especially in evaluating structural capacity and identifying the risk of damage occurring under seismic loads. With the plastic hinge model, a more thorough evaluation of structural damage can be performed, allowing for more effective design improvements and building retrofit.

The pushover analysis results in a capacity curve that illustrates the relationship between base shear and displacement, which are key parameters in assessing the structural performance of a building under lateral loads. This capacity curve, obtained through the FEMA 356 and ATC-40 methods, shows how the structure behaves when subjected to inelastic deformations, with the peak base shear indicating the structural capacity limit and the decline in capacity after the performance point is reached. To ensure the accuracy and validity of the results obtained from the software, the pushover analysis conducted with SAP2000 will be validated through manual calculations. This verification process involves calculating base shear and displacement using the ATC-40 method, with the equations used presented in Equation (1)-(3). By performing manual verification, it can be ensured that the results obtained from SAP2000 are accurate and reliable for evaluating the structural performance of buildings under seismic loads.

$$C_s = \frac{S_a}{T^2} x \left(\frac{1}{1+T^2}\right) \quad (1)$$

$$V = C_s x W \quad (2)$$

$$\Delta = \frac{V}{Ke} \quad (3)$$

Where Cs is dynamic shear coefficient; Sa is spectrum acceleration (g); T is structure period; W is weight of buildings; V is base shear; Ke is effective lateral stiffness; and Δ is displacement.

The period values (T) were obtained from the SAP2000 program, with the regular building having a period of 1.21 seconds, Model A 1.24 seconds, and Models B and C 1.22 seconds. The building weight was calculated based on the total dead load of the structure, additional dead load, and live load, with the regular building weighing 87,928.25 kN, Model A 93,526.12 kN, and Models B and C 92,229.30 kN. The effective lateral stiffness (Ke) was determined based on the total stiffness of the column and beam elements in the structure, which is 42,200.7 kN/m.

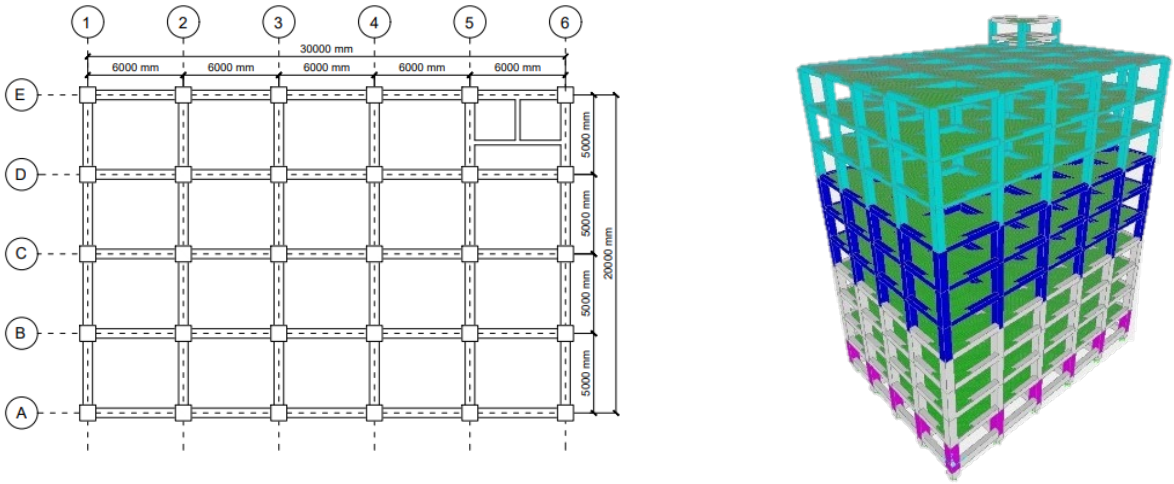

Figure 1 Regular building plan and 3D View

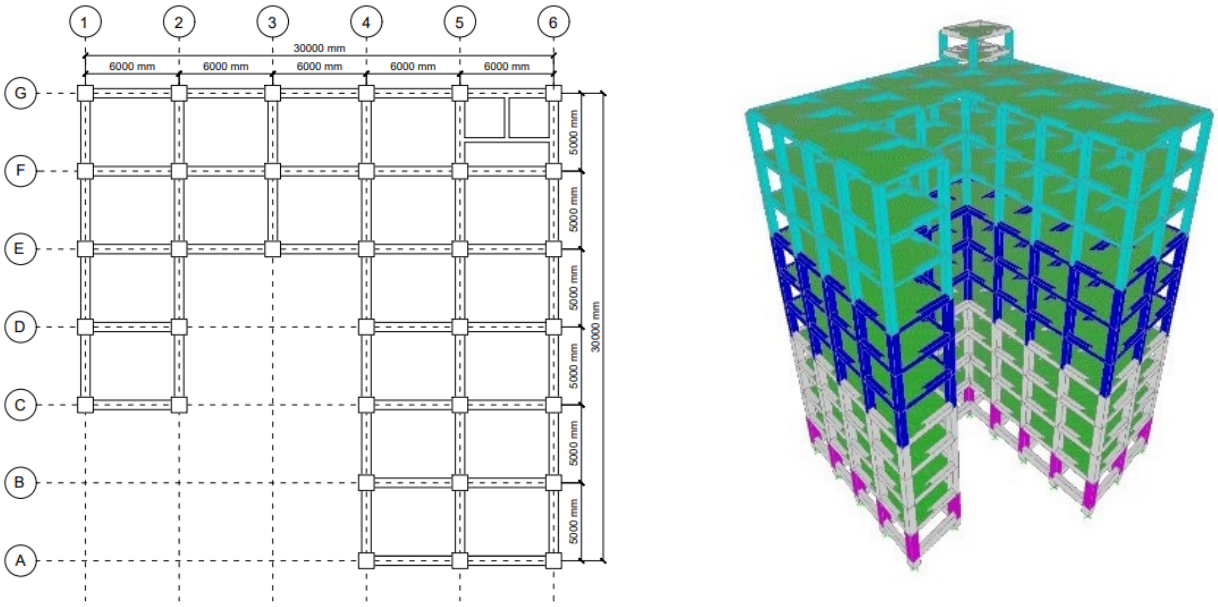

Figure 2 Irregular building plan model A and 3D View

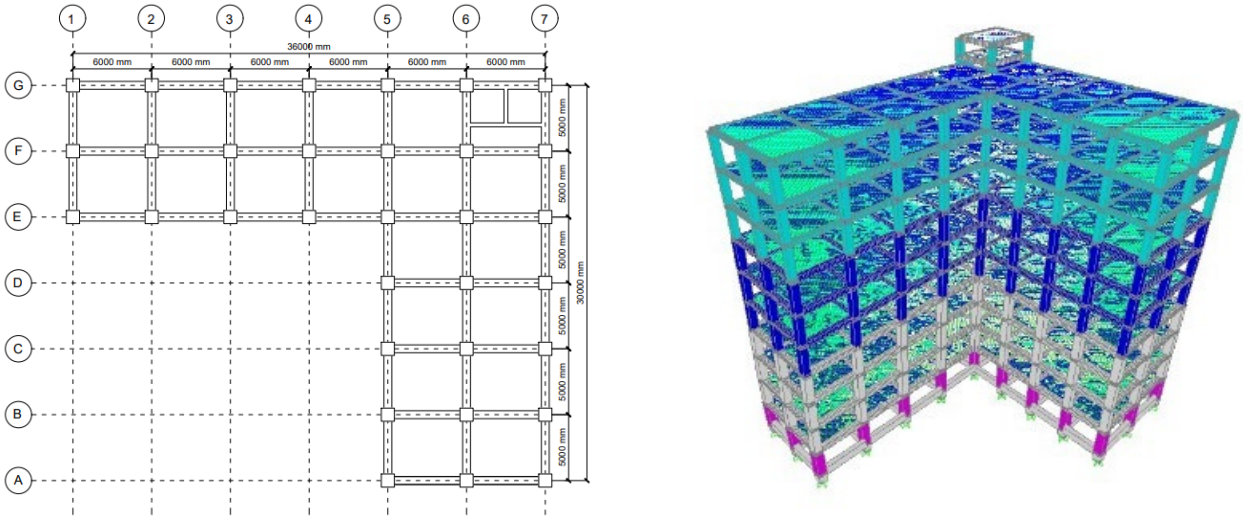

Figure 3 Irregular building plan model B and 3D View

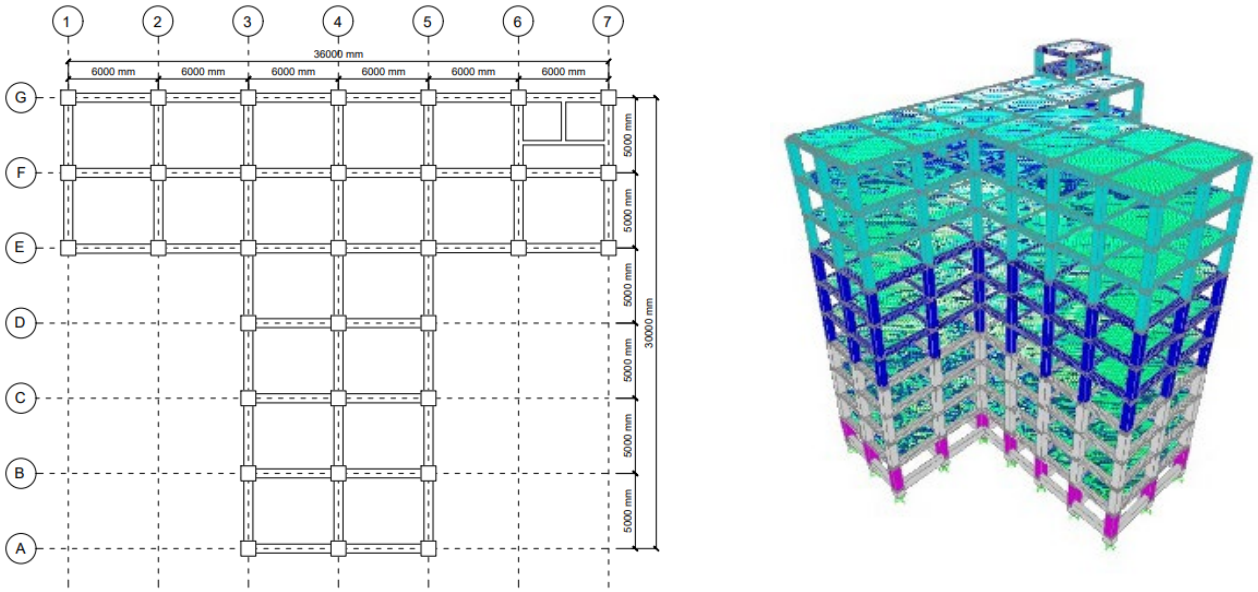

Figure 4 Irregular building plan model C and 3D View

3.0 RESULTS AND DISCUSSION

3.1 Building Eccentricity

The non-uniform column dimensions and irregular structural models result in a gap between the center of mass of the building and the center of stiffness. The gap that arises due to the misalignment of the building center of mass with the center of stiffness is called eccentricity. Building eccentricity can affect the deformation and performance of the building structure.

The analysis results show in Table 3, indicate that Model A (U-shaped) has the largest eccentricity value compared to the other models. The building's eccentricity refers to the distance between the center of mass and the center of stiffness on each floor, which affects the torsional response when lateral loads are applied. On the 10th floor, Model A shows an eccentricity value of 460 mm in the X-direction, significantly larger than Model B and Model C, which show 240 mm and 30 mm values in the X-direction, respectively. The higher eccentricity in Model A indicates that this model exhibits greater torsional eccentricity, contributing to a poorer seismic response. Model A tends to experience more significant torsional effects, resulting in larger displacements in structural elements, particularly in weaker areas such as beams and columns.

These findings align with the research by [18], which shows that buildings with high torsional eccentricity tend to have poorer seismic performance due to uneven forces and greater deformations at the ends of the building. Such irregularities increase torsional stress in the building, leading to faster structural damage, especially in elements far from the center of mass.

3.2 Inter-Level Drift Control

Inter-level drift is a critical parameter in evaluating the safety of buildings under seismic loads. The analysis of inter-story drift was performed according to the requirements of the Indonesian National Standard SNI 1726-2019 [22]Section 7.8.6 stipulates that the maximum allowable drift limit is 2% of the story height for life safety performance. The analysis results indicate that Model A (U-shaped) exhibits the highest drift ratio, reaching 1.44% in the X-direction and 1.30% in the Y-direction, which remains within the maximum limit recommended by SNI 1726-2019 (2% for life safety performance). In comparison, Model B and Model C, which have a more uniform mass and stiffness distribution, show lower drift ratios of 1.3% and 1.1% in the X and Y directions, respectively (see Figure 5).

Model A (U-shaped) is more susceptible to larger inter-story drifts, indicating that this model experiences higher deformation during seismic events. This finding is supported by [19], who confirmed that higher drift ratios in buildings with geometric irregularities often lead to greater structural damage, particularly in elements that undergo plastic deformation.

Nevertheless, the observed drift ratios comply with international standards, such as FEMA 356 and ATC-40. FEMA 356 defines a drift ratio limit of 1% for Immediate Occupancy (IO) and up to 2% for the Life Safety (LS) performance level, while ATC-40 considers the Damage Control (DC) range between 1% and 2%. The drift ratios observed in this study fall within these ranges, aligning with the Damage Control (DC) level according to ATC-40 and approaching the upper limit of Immediate Occupancy (IO) based on FEMA 356 criteria.

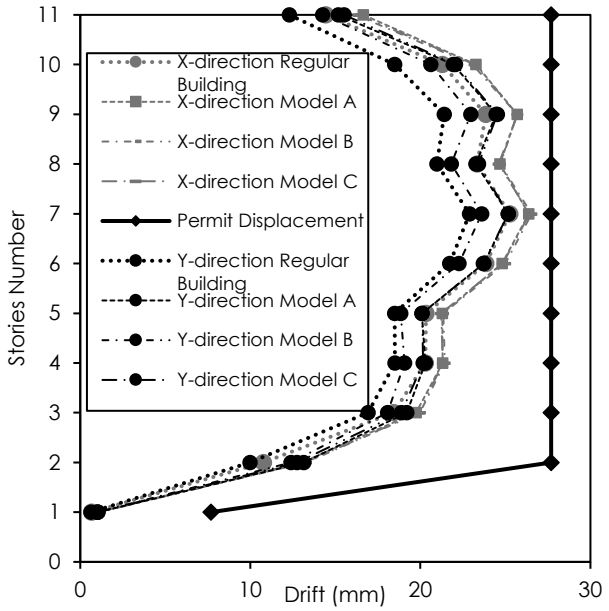

Figure 5 Inter-Story Drift Control

These results are consistent with studies by [18] [6] Which reported drift ratios ranging from 1.2% to 1.8% for similar irregular configurations, confirming that this study's findings align with established literature. However, although Model A meets the standards for life safety performance, the higher deformations could increase the risk of permanent damage to the building, potentially leading to lower structural resilience in the long term.

3.3 Capacity Curve of Pushover Analysis

The result obtained from the pushover analysis is the pushover curve or capacity curve, as illustrated in Figure 6. The capacity curve is formed from the relationship between lateral displacement of the top floor/roof and base shear force, indicating the building's structural performance level. This capacity curve is formed due to the gradual structural push caused by lateral loads with specific loading patterns translated by auxiliary programs. This results in a record of the relationship between base shear and roof displacement. The capacity curve illustrates structural strength, primarily influenced by each structural element's moment deformation capability.

The base shear and displacement results obtained from this study are presented in Table 4 and Figure 7, using the FEMA 356 and ATC-40 methods. The results indicate that the ATC-40 method yields higher base shear and displacement values than the FEMA 356 method. However, both analyses reveal that Model A (U-shaped) exhibits a steeper capacity curve with higher base shear but is also accompanied by larger displacement. This suggests that Model A undergoes greater deformation under higher shear forces. In the capacity curve, Model A shows a higher peak base shear. Still, the structural capacity decreases rapidly after this point, indicating that this model is more vulnerable to faster structural damage once the performance point is exceeded.

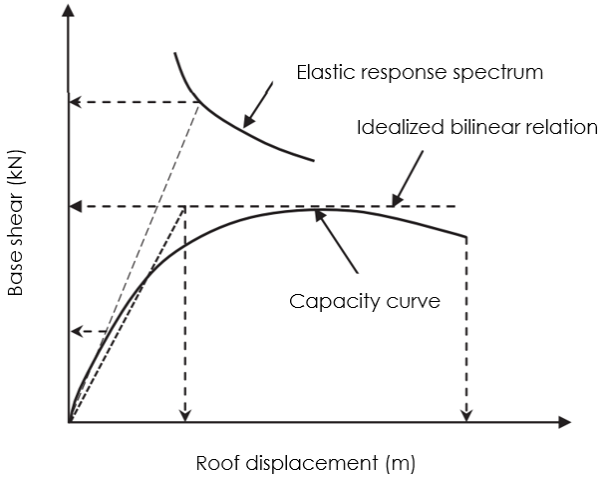

Figure 6 Base shear and roof displacement relationship

In contrast, Model B and Model C display more gradual capacity curves, reflecting a more stable structural response to lateral loads and a more uniform distribution of forces across the structure. These findings align with the study by [19], which showed that buildings with torsional irregularity tend to have sharper capacity curves, leading to increased deformation under high shear forces and a faster decline in structural resilience.

Furthermore, the base shear and displacement results obtained from the pushover analysis were verified through manual calculations using the ATC-40 method, as per Equation (1)-(3). The results of the manual calculation are presented in Table 4 under the section "ATC-40 Manual Analysis", showing that the calculated base shear and displacement values are in close agreement with the results obtained from the pushover analysis. Therefore, it can be confirmed that the analysis results obtained from SAP2000 are valid and reliable for evaluating the structural performance of the building under seismic loads, providing a solid foundation for the use of this software in seismic analysis and earthquake-resistant building design.

3.4 Plastic Hinge of the Structure at the Performance Point

Plastic hinges for all building models were obtained at different displacement stages, as shown in Figure 8. The formation of plastic hinges indicates that the structure has passed the elastic limit and begun the plastic deformation process. The level of plastification is displayed using visual letter codes and colors, where the letter (A) represents the condition where no load has been applied. Thus, no plastification occurs at the plastic hinge. The purple color (B) indicates the condition where the structural element begins to experience initial yielding, the blue color (IO)

represents the stage after yielding (plastic), with the performance level at Immediate Occupancy, the light blue color (LS) represents elements at the Life Safety performance level (plastic condition), the green color (CP) indicates elements at the Collapse Prevention performance level (nearly collapsing condition), the yellow color (C) represents the ultimate capacity of the element, the orange color (D) indicates the residual strength of the element, and the red color (E) represents the condition where the element has already collapsed. The number of plastic hinges formed in the different building models in the X and Y directions is shown in Figure 9-Figure 12.

In the analysis results, Model A (U-shaped) demonstrates faster and more widespread plastic hinge formation than the other models. This process starts in the bottom beams and progressively moves to the columns and upper parts of the structure as the applied loads increase. This behavior aligns with the ductile building mechanism (Strong Column, Weak Beam). The formation of plastic hinges in Model A occurs more rapidly due to the high torsional eccentricity, which leads to increased internal forces at points undergoing deformation, particularly at the structure's ends. In comparison, Model B and Model C show a slower and fewer formation of plastic hinges, indicating that structures with a more uniform stiffness distribution can better resist loads and maintain structural integrity. This finding is consistent with the study by [11], which confirmed that buildings with geometric irregularities exhibit more rapid and frequent plastic hinge formation, suggesting that structures like Model A are more susceptible to early damage.

Table 3 Building Eccentricity

Stories	Regular (mm)		Model A (mm)		Model B (mm)		Model C (mm)	
	X-dir	Y- dir	X-dir	Y- dir	X-dir	Y- dir	X-dir	Y- dir
10	30	30	460	770	240	520	30	210
9	30	30	460	770	240	520	30	210
8	30	30	460	770	240	520	30	210
7	30	30	470	780	250	520	40	210
6	30	30	470	780	250	520	40	210
5	30	30	470	780	250	520	40	210
4	40	40	480	790	260	530	50	220
3	40	40	480	790	260	530	50	220
2	40	40	480	790	260	530	50	220
1	50	50	490	800	270	540	60	230

Table 4 Base shear and displacement

Building Plan	Direction	FEMA 356 (Pushover Result)		ATC-40 (Pushover Result)		ATC-40 (Manual Analysis)	
		Base Shear (kN)	Displacement (m)	Base Shear (kN)	Displacement (m)	Base Shear (kN)	Displacement (m)
Regular	X	17919.36	0.34	20989.84	0.52	20716.59	0.49
	Y	19224.11	0.32	23198.48	0.48	20716.59	0.49
Model A	X	18800.15	0.36	22105.53	0.53	22035.49	0.52
	Y	20742.66	0.30	25115.68	0.47	22035.49	0.52
Model B	X	18706.94	0.34	21993.61	0.52	21729.95	0.51

Building Plan	Direction	FEMA 356 (Pushover Result)		ATC-40 (Pushover Result)		ATC-40 (Manual Analysis)	
		Base Shear (kN)	Displacement (m)	Base Shear (kN)	Displacement (m)	Base Shear (kN)	Displacement (m)
Model C	Y	20254.70	0.32	24706.57	0.49	21729.95	0.51
	X	18706.76	0.34	21953.36	0.52	21729.95	0.51
	Y	20212.11	0.31	24471.45	0.49	21729.95	0.51

Table 5 Story displacement

Stories	Regular (mm)		Model A (mm)		Model B (mm)		Model C (mm)	
	X-dir	Y- dir	X-dir	Y- dir	X-dir	Y- dir	X-dir	Y- dir
Roof	508.27	470.29	540.50	496.27	520.56	493.19	518.87	483.55
10	490.43	454.68	518.54	479.54	500.79	475.77	498.94	466.50
9	463.97	431.04	488.02	454.41	472.45	450.14	470.33	441.16
8	426.89	397.65	446.77	418.96	433.46	414.36	431.09	405.69
7	380.57	355.83	396.18	374.54	385.2	369.78	382.61	361.42
6	325.40	305.56	336.89	321.26	328.23	316.54	325.5	308.47
5	261.59	247.76	270.24	260.13	263.87	255.71	262.05	250.82
4	191.44	185.42	199.68	194.35	195.48	190.45	192.83	188.59
3	121.90	120.08	127.49	125.62	125.92	122.58	122.99	120.49
2	56.13	54.58	58.20	58.05	57.43	56.26	57.08	55.54
1	0.51	0.52	0.57	0.53	0.53	0.54	0.52	0.52

Table 6 Drift ratio

Inter-floor Height (mm)	Regular (mm)		Model A (mm)		Model B (mm)		Model C (mm)	
	X-dir	Y- dir	X-dir	Y- dir	X-dir	Y- dir	X-dir	Y- dir
3600	1.82	1.59	2.24	1.70	2.01	1.77	2.03	1.74
3600	2.69	2.41	3.11	2.56	2.89	2.61	2.91	2.58
3600	3.78	3.40	4.20	3.61	3.97	3.64	4.00	3.61
3600	4.72	4.26	5.15	4.52	4.92	4.54	4.94	4.51
3600	5.62	5.12	6.04	5.43	5.80	5.42	5.82	5.39
3600	6.50	5.89	6.79	6.23	6.56	6.20	6.46	5.87
3600	7.14	6.35	7.19	6.70	6.97	6.65	7.05	6.34
3600	7.08	6.66	7.35	7.00	7.09	6.91	7.11	6.94
3600	6.70	6.67	7.06	6.88	6.98	6.75	6.71	6.62

Inter-floor Height (mm)	Regular (mm)		Model A (mm)		Model B (mm)		Model C (mm)	
	X-dir	Y- dir	X-dir	Y- dir	X-dir	Y- dir	X-dir	Y- dir
3600	5.67	5.51	5.87	5.86	5.79	5.68	5.76	5.60
1000	0.19	0.19	0.21	0.19	0.20	0.20	0.19	0.19

Table 7 Total maximum displacement at the structural performance level

Building Plan	Direction	Height (m)	FEMA 356 Criteria			ATC-40 Criteria		
			δt (m)	Drift Ratio (%)	Performance Level	δt (m)	Drift Ratio (%)	Performance Level
Regular	X	37	0.35	0.93	IO	0.51	1.38	DC
	Y	37	0.31	0.82	IO	0.47	1.28	DC
Model A	X	37	0.36	0.98	IO	0.53	1.44	DC
	Y	37	0.32	0.86	IO	0.48	1.30	DC
Model B	X	37	0.34	0.93	IO	0.52	1.40	DC
	Y	37	0.32	0.87	IO	0.49	1.33	DC
Model C	X	37	0.35	0.93	IO	0.52	1.40	DC
	Y	37	0.32	0.86	IO	0.49	1.32	DC

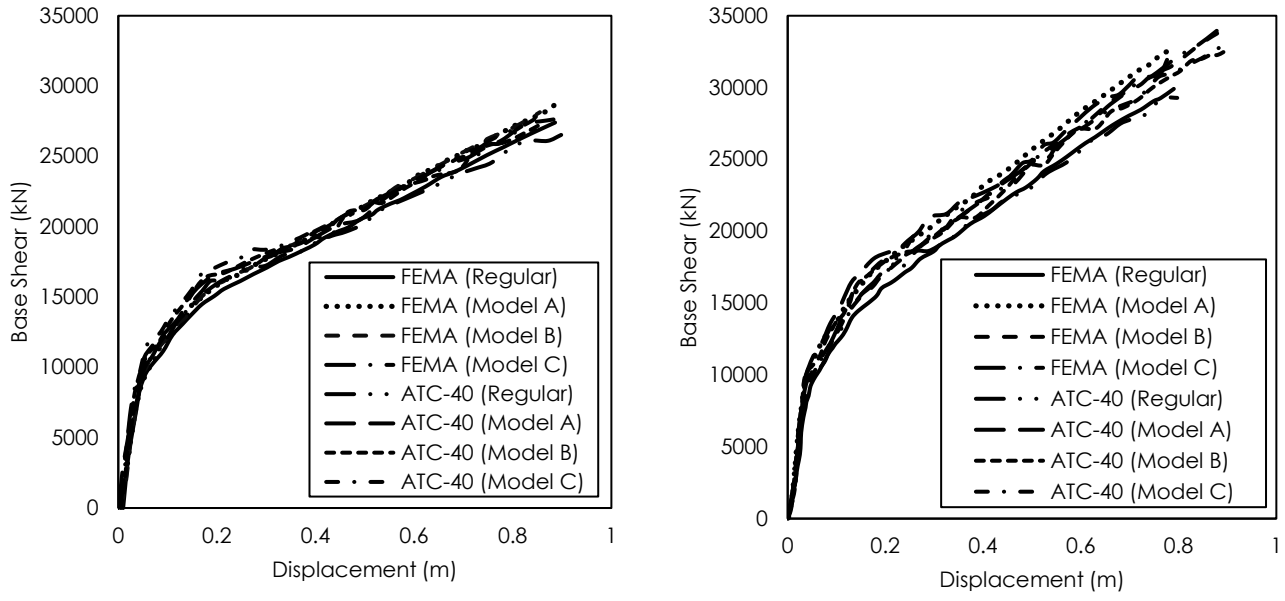

(a) X-direction (b) Y-direction

Figure 7 Capacity curve of pushover result

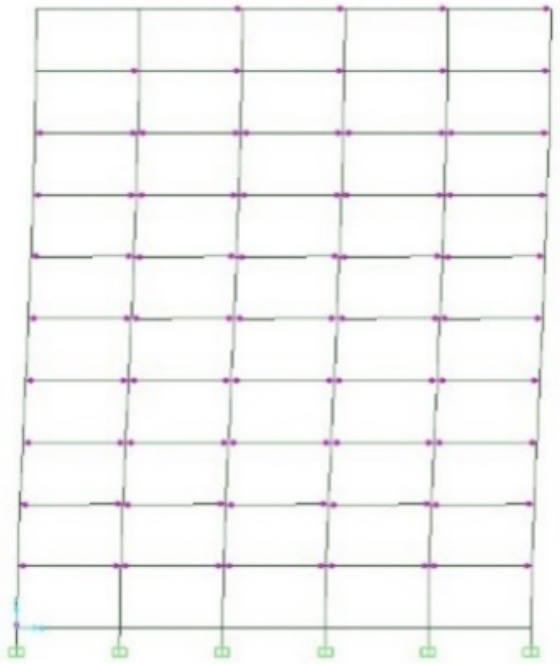

(a) Push-X 14th Steps (Regular Building)

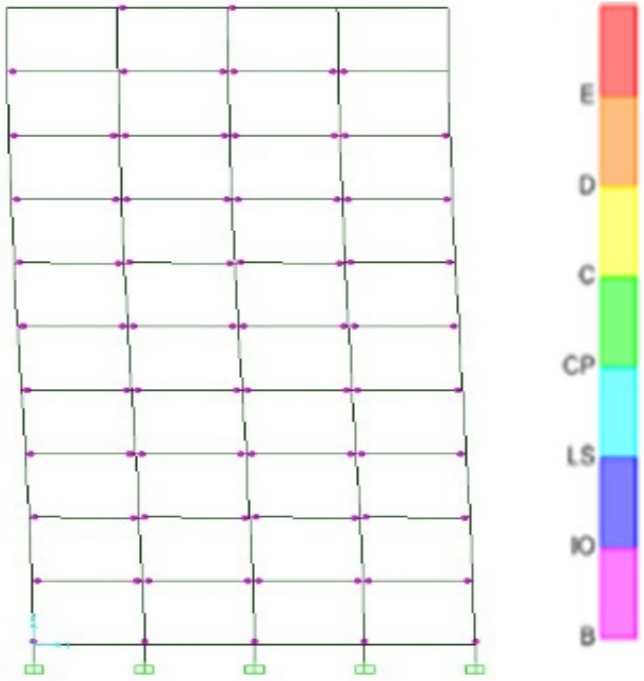

(b) Push-Y 12th Steps (Regular Building)

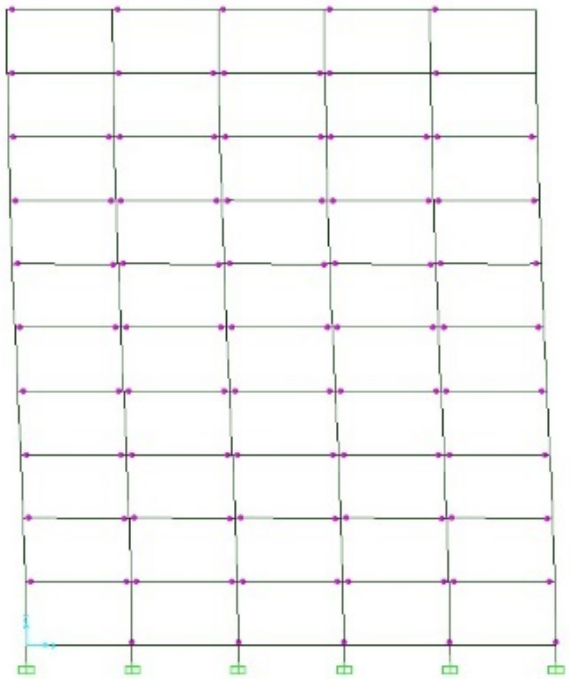

(c) Push-X 10th Steps (Model A)

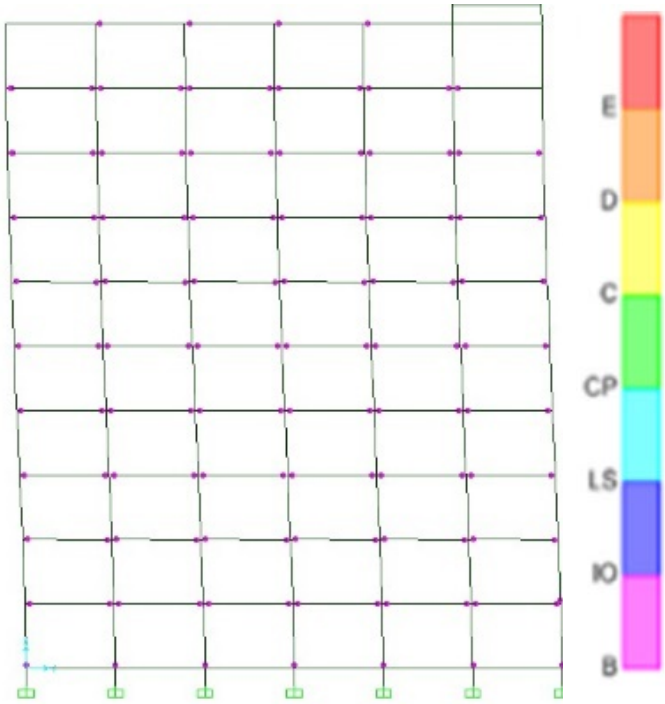

(d) Push-Y 16th Steps (Model A)

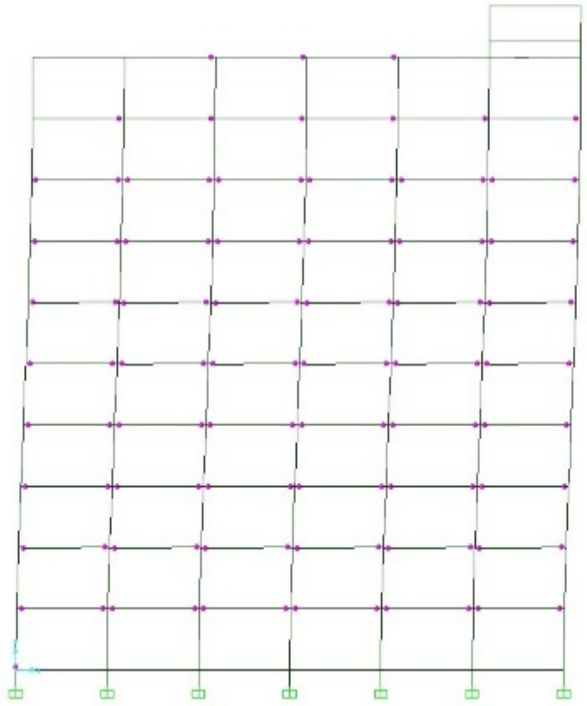

(e) Push-X 12th Steps (Model B)

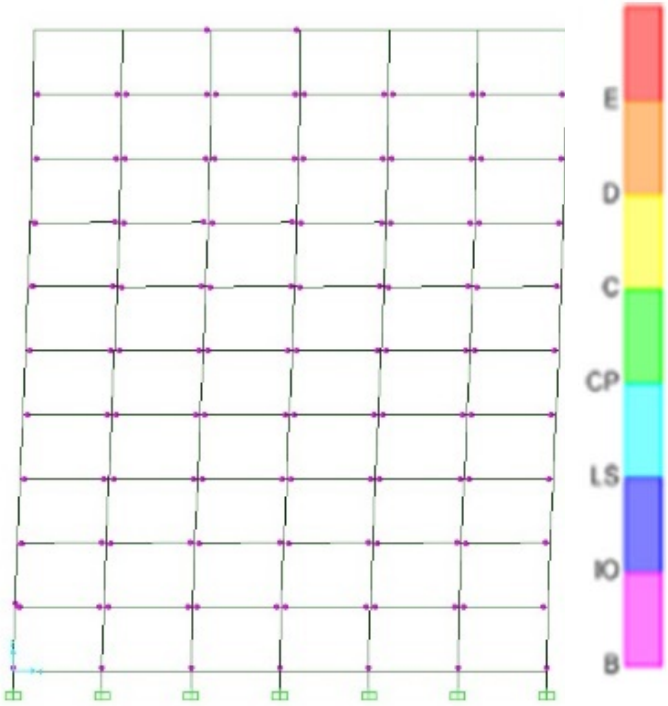

(f) Push-Y 14th Steps (Model B)

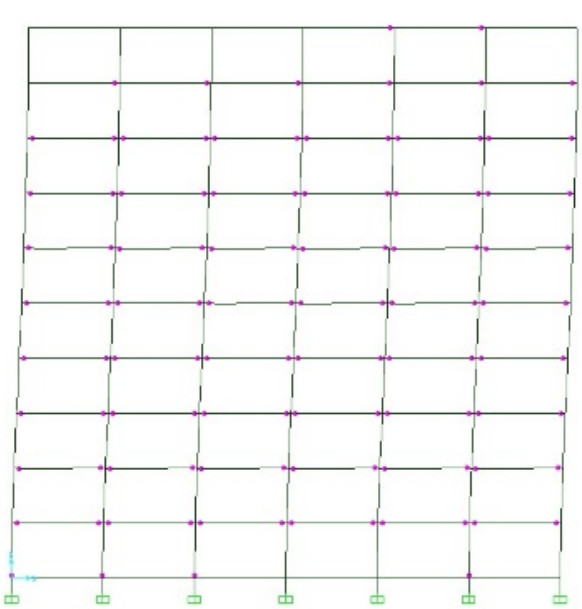

(g) Push-X 11st Steps (Model C)

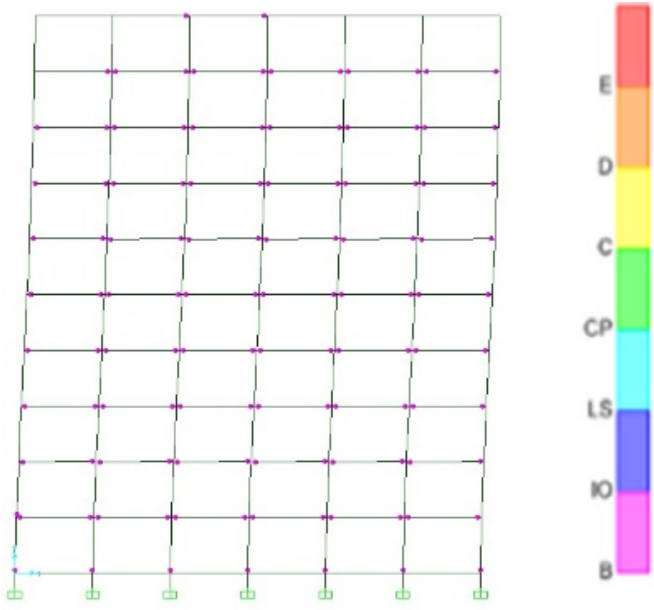

(h) Push-Y 14th Steps (Model C)

Figure 8 Mechanism of plastic hinge formation for the different building plan

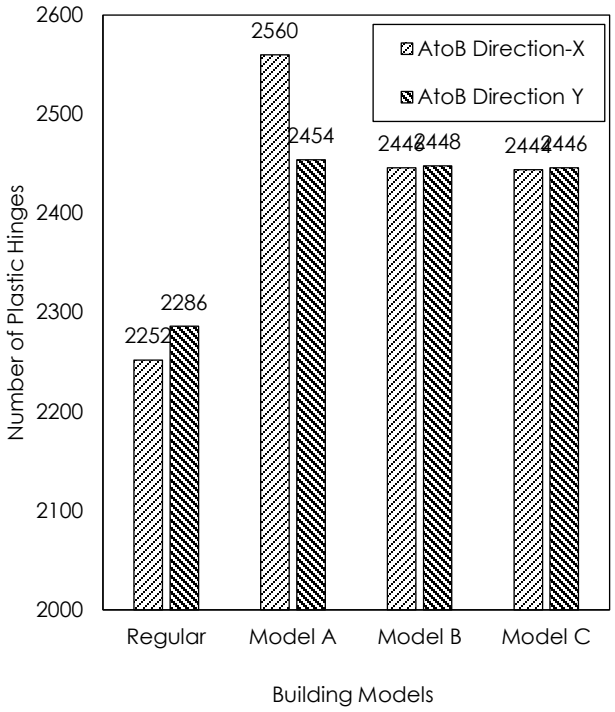

Figure 9 Number of plastic hinges from AtoB

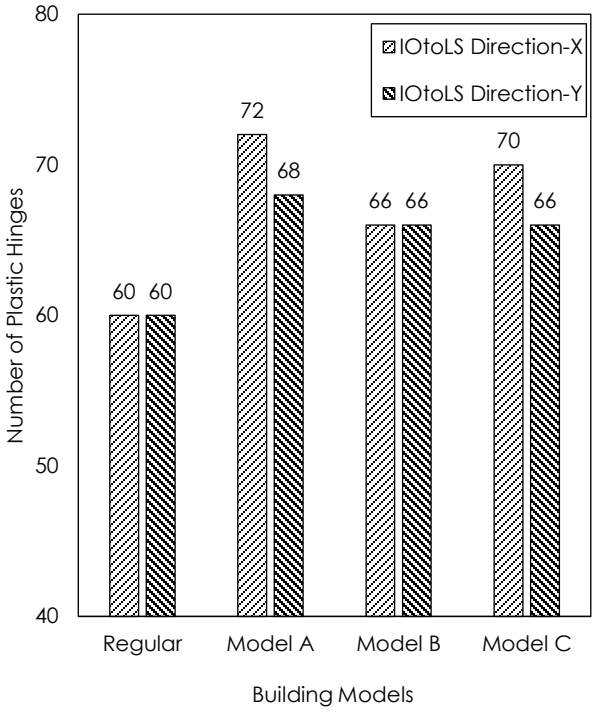

Figure 11 Number of plastic hinges from IOtoLS

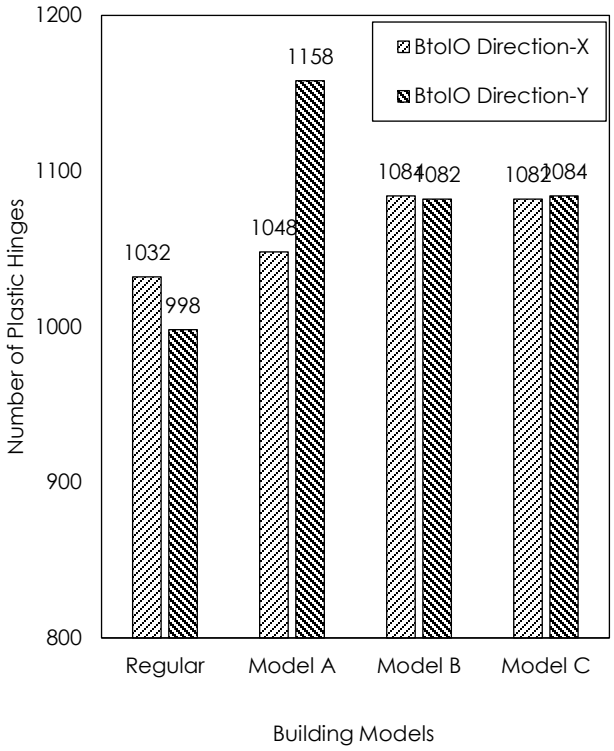

Figure 10 Number of plastic hinges from BtoIO

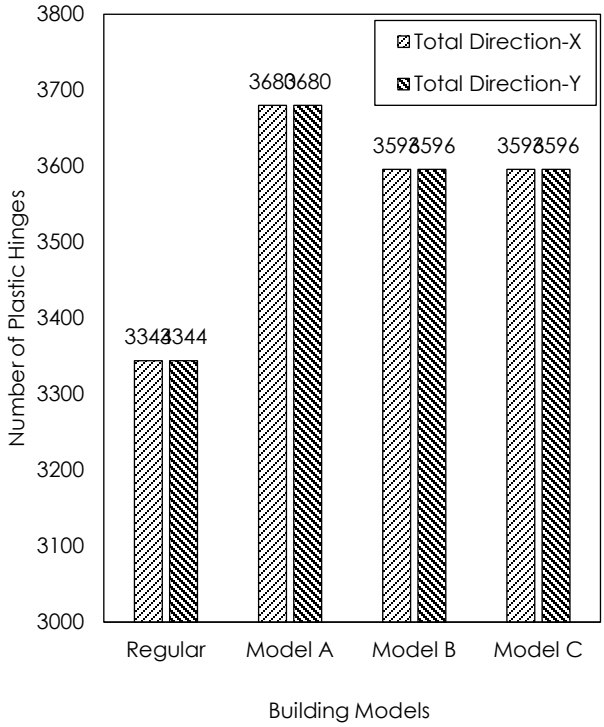

Figure 12 Number of total plastic hinges

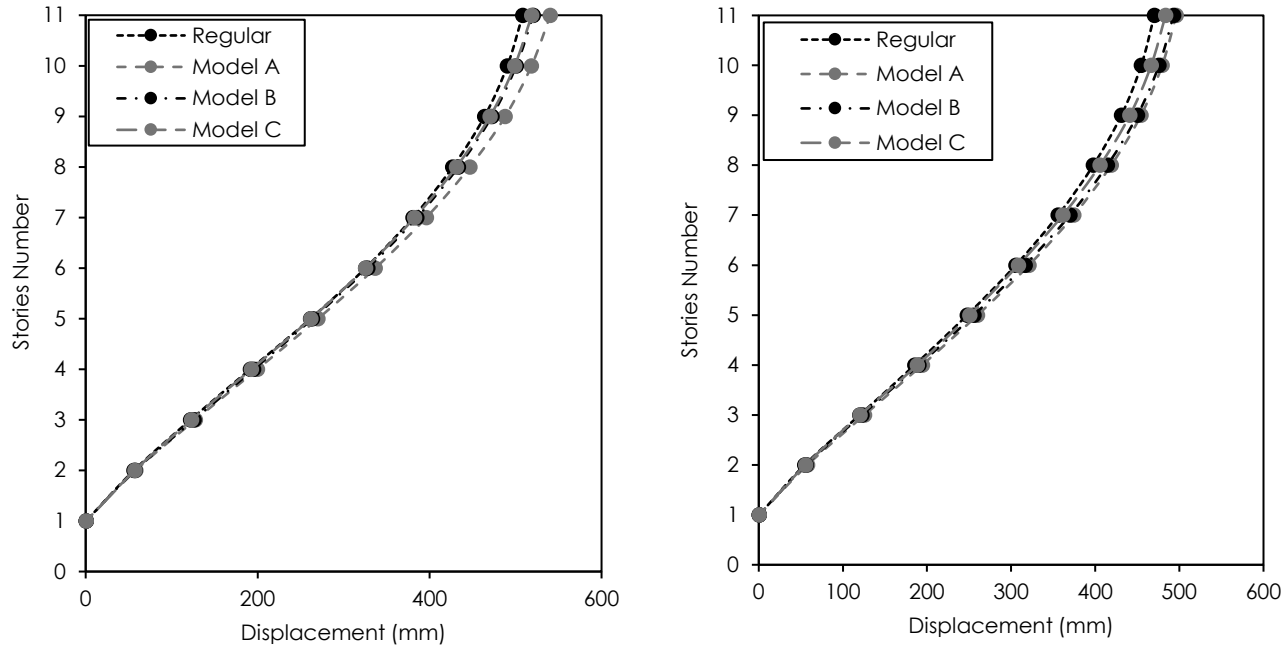

(a) X-direction (b) Y-direction

Figure 13 Story Displacement

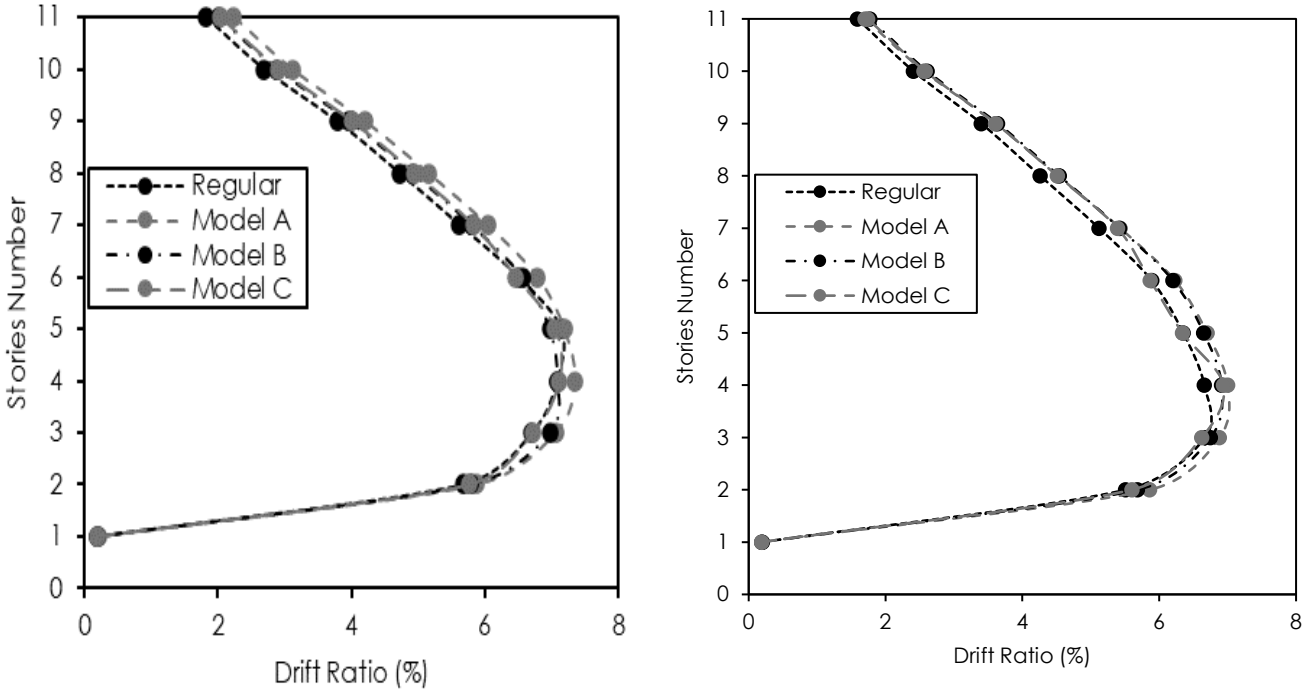

(a) X-direction (b) Y-direction

Figure 14 Drift Ratio

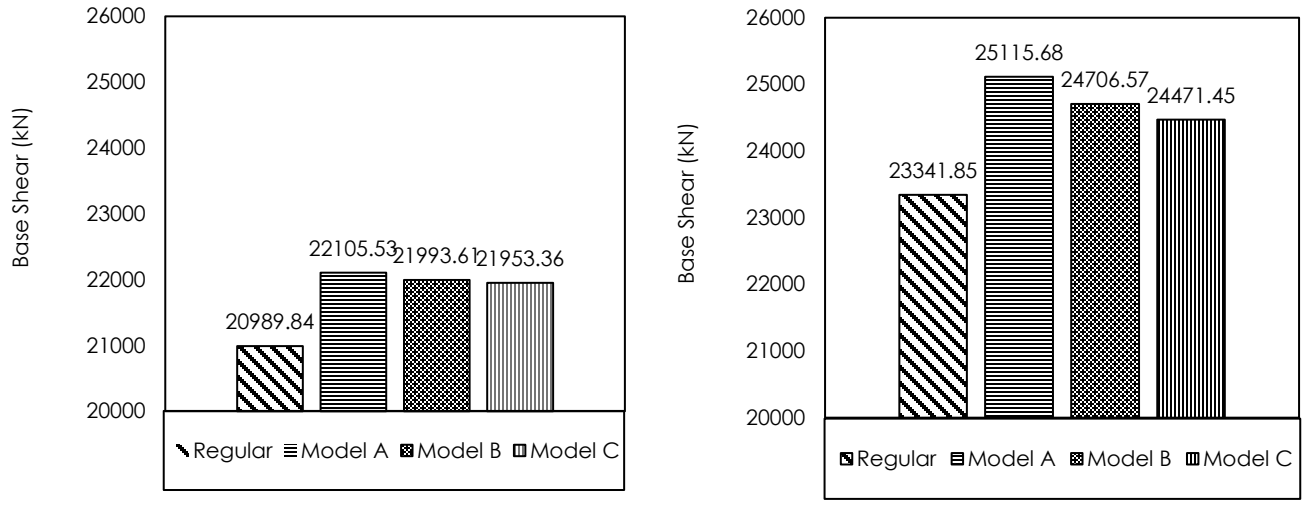

(a) X-direction (b) Y-direction

Figure 15 Base Shear

3.5 Story Displacement

Story displacement measures the lateral displacement at each floor due to lateral loads. The displacement of each floor for all building models was analyzed at the center of mass of the building and recorded at the step where the performance point was reached. The displacement values obtained in this study are presented in Table 4 and Figure 13. The results show that Model A (U-shaped) exhibits the most significant displacement at each floor, reaching 540.50 mm at the roof in the X-direction, which is larger than Model B and Model C, which show displacements of 520.56 mm and 518.87 mm, respectively. These results indicate that Model A experiences greater deformation under seismic loads. The displacement values are consistent with the eccentricity present in each building, as explained in the previous subsection, demonstrating that eccentricity significantly influences the displacement behavior of the structures.

A study by [6] indicates that buildings with irregularities exhibit higher displacements, which can increase the risk of damage to structural elements, particularly beams and columns that experience high shear forces. Therefore, although Model A meets the life safety criteria, the higher displacement levels suggest that this model is more vulnerable to damage in weaker areas, especially at the performance point.

3.6 Drift Ratio

The drift ratio represents the comparison between the inter-story displacement and the story height. The analysis results show that Model A exhibits the highest drift ratios in both directions, with 5.02% in the X-direction and 4.61% in the Y-direction (see Table 6 and Figure 14).

Model B and Model C demonstrate lower drift ratios, reflecting a better structural response to seismic loads. The regular building model shows the lowest drift ratio, indicating that buildings with a more uniform distribution of mass and stiffness respond more efficiently to lateral loads.

As explained in the previous subsection, the observed drift ratios align with the eccentricity present in each building, demonstrating that eccentricity significantly influences the drift ratios occurring in the buildings. This suggests that regular buildings exhibit a more favorable response to earthquake loads.

3.7 Base Shear

The base shear values in Table 8 and Figure 15 Based on the base shear force at the performance point obtained from the pushover curve (ATC-40), the difference obtained represents the comparison of the base shear values between each irregular building and the regular building.

Based on Figure 15, the base shear for Model A is 20,742.66 kN in the Y-direction and 18,800.15 kN in the X-direction, which is higher compared to Model B and Model C. Despite Model A exhibiting higher shear forces, this is not accompanied by a proportional increase in structural performance, as evidenced by the larger displacement and drift ratio. These findings indicate that the torsional effects in buildings with higher irregularity lead to increased base shear, which is not offset by a significant improvement in structural resilience. This is particularly evident in Model A, where the higher base shear is coupled with greater deformation, suggesting that the structural system is more susceptible to failure under seismic loads.

This observation is consistent with the findings of [18] [6], who reported that buildings with greater torsional irregularity often experience higher base

shear values, but their overall seismic performance remains suboptimal due to larger displacements and drift ratios. Similar to these studies, the present analysis underscores the importance of eccentricity in influencing the base shear and displacement, further highlighting the vulnerability of torsionally irregular buildings, particularly regarding structural damage accumulation during seismic events.

Table 8 Base-Shear of the structures

Building Plan	Vx (kN)	Vy (kN)
Regular	20989.84	23341.85
Model A	22105.53	25115.68
Model B	21993.61	24706.57
Model C	21953.36	24471.45

3.8 Performance Level

The structural performance level is determined through the criteria of the roof drift ratio obtained when the target displacement is achieved at performance points. Table 7 Shows the structural performance levels based on FEMA 356 and ATC-40. The roof drift ratio values according to FEMA 356 criteria indicate that they are still less than 1%. Hence, it can be said that based on the drift limits required by FEMA 356, the building performance level at the target displacement is Immediately Occupancy (IO). Meanwhile, the roof drift ratio according to the ATC-40 criteria shows values in the range of 1% - 2%; it can be said that based on the drift limits required by ATC-40, the building performance level at the target displacement is Damage Control (DC). Although the performance levels according to FEMA 356 differ from ATC-40, they have the exact definition. Immediate Occupancy (IO), according to FEMA 356, is a condition where the structure sustains minor damage after an earthquake and can be immediately occupied after an earthquake event. Meanwhile, Damage Control (DC), according to ATC-40, is a condition where the building can still withstand the earthquake, and the risk to human life is very low.

4.0 CONCLUSION

The structural performance of buildings is evaluated based on parameters such as deformation and base shear, which are significantly influenced by the irregularity of the building's plan. Building eccentricity plays a key role in structural performance, where buildings with smaller eccentricity exhibit better structural performance than those with larger eccentricity. The results of this study show that regular buildings perform better than irregular ones, with Model A (U-shaped) irregular buildings exhibiting the poorest structural performance. Model A shows higher base shear and deformation values than other irregular building models, such as Model B (L-shaped), due to its greater eccentricity. This study highlights the importance of understanding the influence of eccentricity on the structural performance of buildings, particularly under seismic loading. The findings emphasize that geometric irregularities, such as those seen in Model A (U-shaped), can worsen structural response, potentially increasing the risk of damage to the building.

To guide seismic-resistant design practices in earthquake-prone regions, the following recommendations are proposed:

- Prioritize regular or symmetric building layouts over highly irregular forms, especially avoiding U-shaped configurations in high seismic zones due to their pronounced torsional effects and displacement demands.
- Enhance seismic detailing at critical joints and connections to ensure ductile failure mechanisms and prevent premature plastic hinge formation.
- Conduct detailed evaluation and strengthening of structural elements subjected to eccentric loading to mitigate the effects of uneven force distribution.
- Incorporate soil–structure interaction (SSI) considerations, particularly for mid- to high-rise structures, to obtain more realistic estimates of drift and displacement.

Although this study provides valuable insight into the behavior of irregular buildings under seismic loading, several areas merit further research. Future investigations should implement nonlinear dynamic time-history analysis to capture better the effects of variable seismic inputs and loading rates. Additionally, the current fixed-base assumption should be replaced with more representative SSI models incorporating realistic foundation flexibility and soil parameters.

Furthermore, the influence of material variability and potential construction imperfections on seismic performance should be analyzed using probabilistic and sensitivity-based approaches. Tailored retrofit strategies are also needed to strengthen existing irregular structures, particularly those exhibiting complex torsional responses, enhancing their resilience and safety in seismic events.

Acknowledgment

The authors thank the Laboratory of Building Materials and Structures of Sepuluh Nopember Institute of Technology for their support in completing this research. The authors gratefully acknowledge financial support from the Institut Teknologi Sepuluh Nopember for this work under the Publication Writing and IPR Incentive Program (PPHKI) 2023 project scheme.

Conflicts of Interest

The authors declare that there is no conflict of interest regarding the publication of this paper.

References

[1] Kuria, K. K., and O. K. Kegyes-Brassai. 2023. Nonlinear Static Analysis for Seismic Evaluation of Existing RC Hospital Building. *Applied Sciences.* 13(21). https://doi.org/10.3390/app132111626.

[2] E, M. G. 2019. Evaluation of Pushover Methodology for Mass-Irregular in Elevation RC Buildings. *Journal of Structural Engineering.* 145(8): 04019082. https://doi.org/10.1061/(ASCE)ST.1943-541X.0002360.

[3] Mahesh, U., and P. Pandit. 2020. A Review on Pushover Analysis for Irregular Structures. 10: 26835–26838.

[4] Indian Standard. 2016. *IS 1893 (Part 1): Criteria for Earthquake Resistant Design of Structures—Part 1: General Provisions and Buildings*.

[5] Pandian, A. V. P., K. P. Arunachalam, A. Bahrami, L. M. B. Romero, S. Avudaiappan, and P. O. Awoyera. 2024. Unsymmetricity Effects on Seismic Performance of Multi-Story Buildings. *Discover Applied Sciences.* 6(9): 476. https://doi.org/10.1007/s42452-024-06099-3.

[6] Divya, R., and K. Murali. 2022. Comparative Analysis of the Behavior of Horizontal and Vertical Irregular Buildings with and without Using Shear Walls by ETABS Software. *Materials Today: Proceedings.* 52: 1821–1830. https://doi.org/10.1016/j.matpr.2021.11.489.

[7] Badan Standardisasi Nasional. 2012. *SNI 1726: Tata Cara Perencanaan Ketahanan Gempa untuk Struktur Bangunan Gedung dan Nongedung*. Jakarta.

[8] Faizah, R., B. Soebandono, and N. M. Iskandar Sugeha. 2021. Acceptability of the Equivalent Static Method for Designing Multi-Story Structures.

[9] Zhang, C., and Y. Tian. 2019. Simplified Performance-Based Optimal Seismic Design of Reinforced Concrete Frame Buildings. *Engineering Structures.* 185: 15–25. https://doi.org/10.1016/j.engstruct.2019.01.108.

[10] Mondal, S., A. K. Rao, and K. Srinivas. 2021. Seismic Performance Assessment of Vertical Irregular Buildings Using Pushover Analysis. *AIP Conference Proceedings.* 2358 (1): 070002. https://doi.org/10.1063/5.0058008.

[11] Mohod, M. V. 2015. Pushover Analysis of Structures with Plan Irregularity. *IOSR Journal of Mechanical and Civil Engineering.* 12(4): 46–55. https://doi.org/10.9790/1684-12474655.

[12] Azizi-Bondarabadi, H., M. Nuno, and P. B. Lourenço. 2021. Higher Mode Effects in Pushover Analysis of Irregular Masonry Buildings. *Journal of Earthquake Engineering.* 25(8): 1459–1493. https://doi.org/10.1080/13632469.2019.1579770.

[13] American Society of Civil Engineers. 2000. *FEMA 356: Prestandard and Commentary for the Seismic Rehabilitation of Buildings*.

[14] Seismic Safety Commission. 1996. *ATC-40: Seismic Evaluation and Retrofit of Concrete Buildings*.

[15] Yurizka, H., and A. Rosyidah. 2020. The Performance of Irregular Building Structures Using Pushover Analysis. *Logic: Jurnal Rancang Bangun dan Teknologi.* 20: 65–72. https://doi.org/10.31940/logic.v20i2.1456.

[16] Guettala, S., I. Abdesselam, A. Y. Rahmani, A. Khelaifia, and S. Guettala. 2025. Advancements in Pushover Analysis for Improved Seismic Performance Evaluation. *Archives of Computational Methods in Engineering*. https://doi.org/10.1007/s11831-025-10278-9.

[17] Aşıkoğlu, A., G. Vasconcelos, P. B. Lourenço, and B. Pantò. 2020. Pushover Analysis of Unreinforced Irregular Masonry Buildings: Lessons from Different Modeling Approaches. *Engineering Structures.* 218: 110830. https://doi.org/10.1016/j.engstruct.2020.110830.

[18] Pandian, A. V. P., K. P. Arunachalam, A. Bahrami, L. M. B. Romero, S. Avudaiappan, and P. O. Awoyera. 2024. Unsymmetricity Effects on Seismic Performance of Multi-Story Buildings. *Discover Applied Sciences.* 6(9). https://doi.org/10.1007/s42452-024-06099-3.

[19] Yurizka, H., and A. Rosyidah. 2020. The Performance of Irregular Building Structures Using Pushover Analysis. *Logic: Jurnal Rancang Bangun dan Teknologi.* 20(2): 65–72. https://doi.org/10.31940/logic.v20i2.1456.

[20] Divya, R., and K. Murali. 2022. Comparative Analysis of the Behavior of Horizontal and Vertical Irregular Buildings with and without Using Shear Walls by ETABS Software. *Materials Today: Proceedings.* 52: 1821–1830. https://doi.org/10.1016/j.matpr.2021.11.489.

[21] Standar Nasional Indonesia. 2020. *SNI 1727: Beban Desain Minimum dan Kriteria Terkait untuk Bangunan Gedung dan Struktur Lain*.

[22] Standar Nasional Indonesia. 2019. *SNI 1726: Tata Cara Perencanaan Ketahanan Gempa untuk Struktur Bangunan Gedung dan Nongedung*.

[23] Zameeruddin, Mohd., and K. K. Sangle. 2021. Performance-Based Seismic Assessment of Reinforced Concrete Moment Resisting Frame. *Journal of King Saud University – Engineering Sciences.* 33(3): 153–165. https://doi.org/10.1016/j.jksues.2020.04.005.